Stress Wave Anisotropy in Centered Square Highly Nonlinear Granular Systems

A. Leonard and C. Daraio

Stress wave anisotropy in centered square highly nonlinear granular systems

A. Leonard and C. Daraio

Graduate Aerospace Laboratories (GALCIT) California

Institute of Technology, Pasadena, CA 91125, USA

Abstract

Highly ordered, close packed granular systems present a nonlinear dynamic behavior stemming from the Hertzian contact interaction between particles. We investigated the propagation of elastic stress waves in an uncompressed, centered square array of spherical and cylindrical particles. We show, via experiments and numerical simulations, that systematic variations of the mass and stiffness ratios of the spherical and cylindrical particles lead to large variations in the characteristics of the propagating stress wave fronts traveling through the system. The ability to control the stress wave front properties in these granular systems may allow for the development of new wave-tailoring materials including systems capable of redirecting impact energy.

PACS numbers: 05.45.-a, 45.70.-n, 46.40.Cd

Granular systems composed of particles arranged in a tightly packed lattice-like configuration, present a nonlinear dynamic behavior originating from the Hertzian contact interaction between particles. Extensive studies have shown that uniform one-dimensional granular systems support the formation and propagation of solitary waves with unique properties [1–3]. In addition, several works have exploited the properties of these solitary waves at granular boundaries in order to design one-dimensional impulse mitigating devices [4, 5]. While the transient dynamic response of one-dimensional highly nonlinear (uncompressed) granular chains has been extensively studied, few reports have explored wave propagation in two-dimensional ordered granular systems.

Several previous studies focused on the role of force chains in the dynamic load transfer path in disordered or moderately ordered granular systems [6, 7]. Zhu et al. studied how the packing of photoelastic disks affected the dynamic load transfer path in two-dimensional systems. More recently, Nishida and Tanaka looked at the force profile transmitted through two-dimensional hexagonal packing of spheres impacted by a spherical projectile. They determined that the transmitted force could be reduced by increasing the number of layers in the system, or by introducing a dissimilar material layer [8]. Regarding the ability to redirect stress wave energy, more complex y-shaped granular systems have shown the ability to split and recombine incident pulses [9].

The study of two-dimensional systems enables the discovery of novel physical phenomena not possible in one-dimensional systems, for example, spatial redirection and anisotropic energy trapping. This work studies the propagation of elastic stress waves in highly nonlinear (uncompressed), uniformly packed, two-dimensional granular systems subject to impulsive loading. While several past works investigated the wave propagation in highly nonlinear two-dimensional granular systems [8, 10, 11], here we show the ability to systematically alter the shape of the stress wave front propagating in the granular system, through experiments and numerical simulations.

The granular systems studied in this work consisted of an uncompressed 20 by 20 square array of spherical particles that contains a 19 by 19 square array of cylindrical particles (intruders) in the interstitial spacings. The diameter of the cylindrical particles was selected to allow a tight fit in the interstitial spaces (Figure 1). By varying the stiffness and mass ratios of the spherical and cylindrical particles, we observed a wide range of wave front shapes indicating substantial impact energy redirection. Numerical simulations on extended
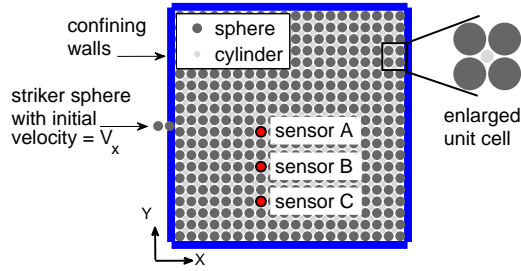
Figure 1: Schematic diagram of the experimental setup. The striker sphere impacted a resting striker sphere located between the 10th and 11th spherical particles along the edge. Sensors A, B, and C are located at positions X_8Y_{10}, X_8Y_7, and X_8Y_4 of the 20 by 20 spherical square array, respectively.

systems with similar geometries are being performed by collaborators [15].

In the absence of cylindrical intruders, previous studies showed that the square array supported the formation and propagation of solitary waves along only initially excited chains [12]. The solitary waves traveling in this simple square packing were shown to have similar properties to the solitary waves observed in one-dimensional systems [12]. The addition of cylindrical intruders in the simple square packing transforms the system's response from quasi-one-dimensional to a truly two-dimensional response. The introduction of additional contact points between the particles enables lateral energy redistribution. The lateral stress propagation properties depend on the mass and elastic properties of the intruder particles, as compared to the spherical particles. Variations of the particles' properties lead to variations in the stress propagation front within the system. For selected configurations, the wave front shape was highly directional, or triangular, in which most of the energy was directed centrally, in-line with the impact direction (similar to the case without intruders). For other material configurations, the wave front shape was significantly spread along oblique directions, redirecting the impact energy towards the system's edges (see Figure 2).

Experiments were performed on granular systems assembled within a confining box. Custom-fabricated sensor particles, instrumented with miniature tri-axial accelerometers, replaced solid spheres at selected locations within the system (Figure 1). Refer to [12] for a detailed description of the experimental setup and sensor particles. Spherical particles were 19.05 mm in diameter and cylindrical particles were 7.89 mm in diameter and 19.05 mm

in length. Spheres were either stainless steel (type 316) with Young's Modulus $E = 193$ GPa, Poisson's ratio $\nu = 0.3$, and mass $m = 29.0g$ or delrin, with $E = 3.1$ GPa, $\nu = 0.35$, and $m = 5.1g$ [12]. Cylinders were either stainless steel (type 316), $m = 7.5g$ or polytetraflouroethylene (ptfe), with $E = 0.5$ GPa, $\nu = 0.46$, and $m = 2.0g$ [3, 12].

Numerical simulations utilized a two-dimensional discrete particle model, in which each particle was modeled as a point mass connected by nonlinear springs at the contacts. The well known Hertzian [13] force-displacement relationship, $F = k\Delta^{3/2}$, was used to model the nonlinear springs, where F is the force, k the stiffness coefficient, and Δ the displacement between the center of two particles in contact. The stiffness coefficient for two spherical particles (i and j) in compression can be described by :

$$k_{sphere_i, sphere_j} = \frac{4}{3} A_{i,j}^{-1} \left(\frac{R_i R_j}{R_i + R_j} \right)^{\frac{1}{2}} \tag{1}$$

where R is the radius of each sphere and $A_{i,j} = \left(\frac{1-\nu_i^2}{E_i} + \frac{1-\nu_j^2}{E_j} \right)$. In the case of a sphere and cylinder in compression, the same $3/2$ power-law can be used, but with a slightly modified stiffness coefficient:

$$k_{sphere_i, cylinder_j} = A_{i,j}^{-1} (2eR_i)^{\frac{1}{2}} K^{2/3} \tag{2}$$

where e and K are tabulated functions of the sphere and cylinder radii, R_i and R_j, and can be found in [14]. Simulations used a fourth order Runge-Kutta scheme to integrate the equations of motion following from the above relationships, similar to [1, 9, 12] but with the addition of the sphere-cylinder force-displacement stiffness coefficient (Equation 2). Dissipative terms were not included in the simulations. We used experimentally measured impact velocities as input in the simulations.

We performed experiments and numerical simulations for four different sphere-cylinder material combinations: (a) steel-ptfe, (b) delrin-ptfe, (c) steel-steel, and (d) delrin-steel. Previous works have observed significant variability in experimental data on two-dimensional granular systems as a result of imperfections in the contact lattice [11]. To address the effects of imperfections, we assembled each material configuration, (a) through (d), three times and 15 experiments were performed for each initial contact lattice. In this way, we captured the variability between successive experiments on the same granular system, in addition to the variability as a result of differences in the systems' initial contact lattices. When comparing experiments with numerical simulations incorporating disorder, we observed that variations
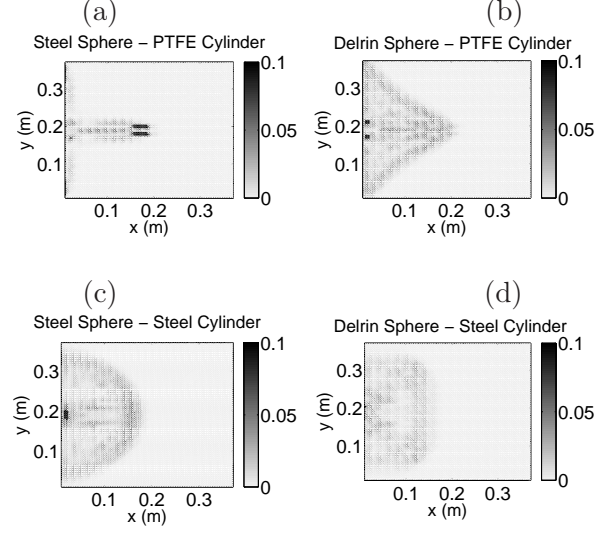
Figure 2: Numerical simulation results showing the wave front shape in terms of particle velocity magnitude for each of the experimentally tested material configurations. X- and Y-axes represent the particle position. For the steel sphere configurations, Figures (a) and (c) show particle velocities 0.35 ms after the steel striker sphere impact ($V_x = 0.73$ m/s). For the delrin sphere configurations, Figures (b) and (d) show particle velocities at 1.0 ms after the delrin striker sphere impact ($V_x = 0.92$ m/s). Grey scales indicate particle velocity in m/s.

from the systems' ideal response can be primarily attributed to radii imperfections which create disorder in the contact lattices. However, on average, the response of all systems is consistent with the ideal systems' response [15].

The numerical simulations presented in this letter always assumed a perfect contact lattice. The numerical results showed significant differences in the wave front shape, in terms of particle velocity magnitude, between each of the tested material configurations (Figure 2). When the tested system consisted of stiff, heavy spheres and light, softer intruders, we observed highly directional wave propagation (Figure 2a). When the tested system consisted of slightly stiffer spheres than cylinders with similar masses, we again observed a wave front in which most of the energy was directed centrally in-line with the impact, but with a more uniform triangular shape (Figure 2b). The configuration of spheres and cylindrical intruders of identical materials resulted in a relatively uniform, circular wave front propagating through the granular system (Figure 2c). Lastly, when we tested the system composed of light, soft spheres with heavier, stiff intruders we were able to divert a
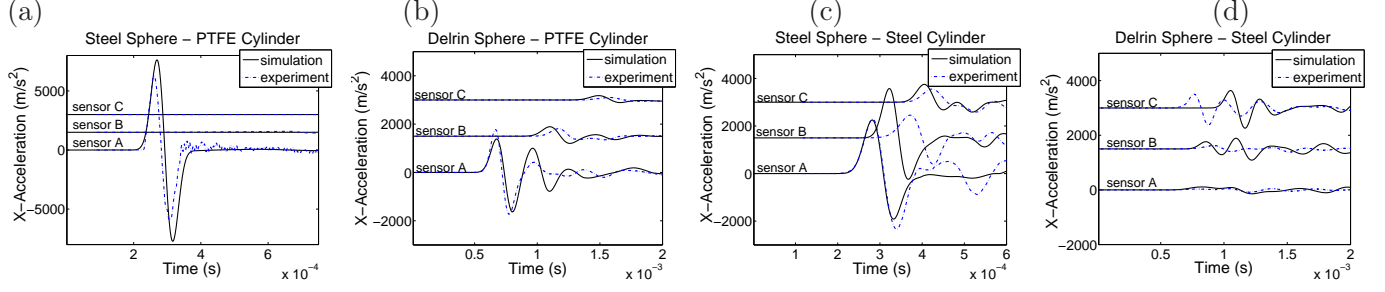
Figure 3: Comparison of individual particle acceleration as a function of time between experiments and simulations for each of the sphere-cylinder material combinations tested: (a) steel-ptfe, (b) delrin-ptfe, (c) steel-steel, and (d) delrin-steel. Acceleration data at sensor locations B and C were shifted up 1500 and 3000 m/s^2, respectively for visual clarity. Zero time in simulations was defined as the moment of striker impact. To compare experimental and simulation data, experimental data for each test configuration was shifted so the signal arrival time of sensor A in simulations and experiments coincided.

significant portion of the impact energy towards the system's edges, away from the central particles (Figure 2d).

We can describe the differences in the propagating wave front in terms of relative arrival times and relative stress wave amplitudes within the granular systems. The relative arrival times of the wave front at locations parallel to the y-axis can be used to describe the wave front shape. Additionally, the relative amplitudes along the same line can be used to describe the distribution of energy in the wave front. However, a unique property of nonlinear granular systems is that these two quantities are not independent. Several previous studies [2, 3] have verified Nesterenko's amplitude dependent wave speed relationship for a highly nonlinear, one-dimensional granular chain of spherical particles [1]. For more complex two-dimensional systems the exact analytical relation between wave speed and amplitude is not known. However, in our experiments and numerical simulations we observe that directions of higher wave amplitude will also be directions of faster wave propagation.

The characteristics describing the different wave shapes observed in numerical simulations are in good agreement with the experimental data (Figure 3). The experimental data in Figure 3 represents the typical response of each system (i.e. is representative of the mean values plotted in Figure 4 (Top) for a single packing). We present here only the x-acceleration, however, we observed that the comparison between experiments and numerical simulations

of both x- and y-acceleration displayed consistent trends. For the system composed of steel spheres and ptfe intruders, we observed most of the impact energy being centrally directed, in-line with the impact, and we detected negligible signals away from the central particles, in excellent agreement with numerical simulations (Figure 3a). In the system consisting of delrin spheres and ptfe intruders (Figure 3b), we observed a considerably higher amplitude signal arriving first at the central sensor, as opposed to the signal detected towards the system's edges. These differences in amplitude and arrival times measured between sensors qualitatively agree with the numerical results showing the formation of a triangular wave front shape. For the case of identical sphere and intruder particle materials (Figure 3c), we observed comparable amplitudes at central sensors, A and B (see Figure 1), with slightly lower amplitude at the sensor closer to the system's edge. We also observed relative signal arrival times consistent with the numerically observed more uniform, rounded wave front. Finally, by using delrin spheres and steel intruders, we observed the largest amplitude signal furthest from the central particles (Figure 3d) indicating substantial impact energy redirection, consistent with the numerical simulations.

In the lattices that incorporate stiffer intruders, deviations were apparent between the experimental and numerically calculated signal amplitudes and arrival times (Figure 3c,d). The presence of dissipation, evident in the experimental results, may account for the noticeable time delays observed between the pulses recorded experimentally and the ones obtained from numerical simulations. A notable discrepancy between experiments and numerical simulations exist in the relative signal arrival times in the case of delrin spheres and steel cylinders (Figure 3d); the experiments seem to suggest an exaggerated impact energy redirection.

To quantify the variability of the experimentally measured response in the different physical packings, we analyzed the wave front amplitude distributions and compared them with numerical simulations for each of the material configurations (Figure 4). We calculated the ratio of the maximum amplitude at sensor location C with respect to location A (Figure 1), capturing the main features of the wave fronts. An amplitude ratio greater than one, as observed with the delrin spheres and steel intruders, indicates a wave front consistent with the impact energy being diverted away from the central line of impact. A ratio near one, as observed for the steel spheres and steel intruders, indicates a uniform, circular wave front. Similarly, as the ratio decreases below one we observed more amplitude being centrally directed within the system. While there is notable variation between experiments, the
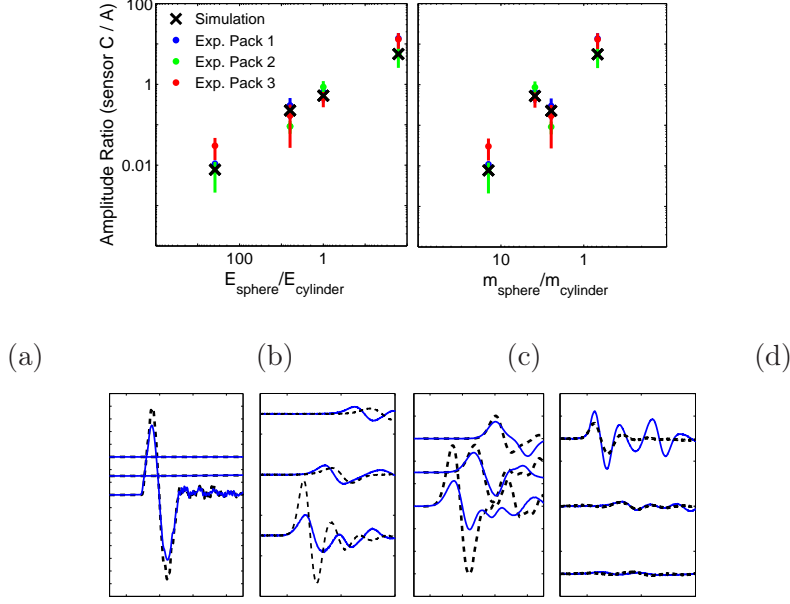
Figure 4: (Top) Ratio of the maximum acceleration amplitude at sensor locations C and A plotted against the ratio of the sphere-cylinder (Left) stiffness and (Right) masses. For experimental data, the mean and standard deviation, std, (error bars) are plotted for each of the three initial packings assembled for each material configuration. (Bottom) The x-accelerations at sensor locations A, B, and C (positioned as in Figure 3) most closely representing +1 std (solid blue) and -1 std (dashed black) for Pack 1 are plotted for each sphere-cylinder material configuration: (a) steel-ptfe, (b) delrin-ptfe, (c) steel-steel, and (d) delrin-steel. Y-ticks indicate $1000\ m/s^2$. X-ticks indicate 0.1 ms for (a) and (c) and 1.5 ms for (b) and (d).

agreement between the mean response in experiments and numerical simulations is quite good. To visualize the variation in wave front shapes between successive experiments, the experiments most closely representing the standard deviations are also plotted for a packing of each test configuration (Figure 4 Bottom).We plotted the wave front amplitude ratio against both the sphere-cylinder material stiffness ratio and mass ratio (Figure 4 Top). A decreasing trend was observed for both stiffness and mass ratios as the wavefront began to follow a more pointed triangular form. However, only the stiffness ratio had a monotonically decreasing relationship with the shape of the particle velocity wave front. This suggests that the material stiffness had a more significant effect on the wave front shape than the mass ratios for the material combinations tested.

We performed additional numerical simulations with different impact velocities and observed that the wave front shape in the highly nonlinear regime is independent of excitation amplitude (within the elastic limit). The properties of the traveling waves depend on the relative size of the excitation to the initial displacement, or pre-compression. We performed additional numerical simulations on the presented granular systems with pre-compression, in which we varied the impact velocity (i.e. varied the regime from linear, to weakly nonlinear, to highly nonlinear). We found that in all cases, the general wave front shape is consistent with those described by the uncompressed regime. However, as the system moves toward the linear regime the effects of dispersion become prominent, and more of the energy is distributed into the trailing waves as opposed to more energy being carried in the wave front in the highly nonlinear regime studied here.

In conclusion, we demonstrated the ability to systematically alter the shape of the stress wave front traveling through a two-dimensional granular system subject to impulse loading. By varying the mass and stiffness ratios of the particles in the array, we showed extensive variation in the wave front shape resulting in substantial impact energy redirection. Experimental results confirmed the variation in wave shape observed in numerical simulations in terms of the wave front amplitude distribution. The ability to control the stress wave front properties in granular systems may allow for the development of new wave-tailoring materials which could be used, for example, as protective layers capable of redirecting and trapping mechanical energy.

[1] V. F. Nesterenko, *Dynamics of Heterogeneous Materials* (Springer-Verlag, New York, NY, 2001).

[2] C. Coste, E. Falcon, and S. Fauve, Phys. Rev. E **56**, 6104 (1997).

[3] C. Daraio, V.F. Nesterenko, E.B. Herbold, and S. Jin, Phys. Rev. E **72**, 016603 (2005).

[4] C. Daraio, V.F. Nesterenko, E.B. Herbold, and S. Jin, Phys. Rev. Lett. **96**, 058002 (2006).

[5] R. Doney and S. Sen, Phys. Rev. Lett. **97**, 155502 (2006).

[6] S. Bardenhagen and J. Brackbill, J. Appl. Phys. **83**, 5732 (1998).

[7] K. Roessig, J. Foster, and S. Bardenhagen, Exp. Mech. **42**, 329 (2002).

[8] M. Nishida and Y. Tanaka, Granular Matter **12**, 357 (2010).

[9] C. Daraio, D. Ngo, V.F. Nesterenko, and F. Fraternali, Phys. Rev. E **82**, 036603 (2010).

[10] Y. Zhu, A. Shukla, and M. Sadd, J. Mech. Phys. Solids, **44**,1283 (1996).

[11] B. Gilles and C. Coste, Phys. Rev. Lett. **90**, 174302 (2003).

[12] A. Leonard, F. Fraternali, and C. Daraio, Exp. Mech. (online Doi: 10.1007/s11340-011-9544-6).

[13] K. Johnson, *Contact mechanics* (The Press Syndicate of the University of Cambridge, 1987).

[14] M. Puttock and E. Thwaite, *Elastic Compression of Spheres and Cylinders at Point and Line Contact*, CSIRO: Melbourne (1969).

[15] A. Leonard, A. Awasthi, P. Geubelle, and C. Daraio, (in progress).